

LAMINAR BOUNDARY LAYERS OF CO-CURRENT GAS-LIQUID STRATIFIED FLOWS—II. VELOCITY MEASUREMENTS

PL. MITEV and CHR. BOYADJIEV

Central Laboratory for Chemical Engineering, Bulgarian Academy of Sciences, Geo Milev, bl. 5, Sofia 13,
Bulgaria

(Received 21 July 1975)

Abstract—An experimental investigation of the velocity distribution in the laminar boundary layer at a moving interface in co-current gas-liquid flow has been made. The velocity profiles were measured by hot wire technique at different distances from the initial phase interaction location. The experimental results compare well with theoretical predictions which are solutions of the Prandtl's equations.

1. INTRODUCTION

Boyadjiev *et al.* (1976), hereafter referred to as Part I, has shown that the velocity distribution in the gas and the liquid phase can be represented† by means of two dimensionless functions:

$$u_G = U_G^\infty f'(y \sqrt{U_G^\infty / \nu_G x}); \quad u_L = U_L^\infty \varphi'(-y \sqrt{U_L^\infty / 4 \nu_L x}), \quad [1]$$

where f' and φ' can be obtained from "exact" numerical solution of the Prandtl equations for different values of the parameters $\theta_1 = U_L^\infty / U_G^\infty$ and $\theta_2 = (\mu_G / \mu_L)(\nu_G / \nu_L)^{-1/2}(U_G^\infty / U_L^\infty)^{3/2}$, as well as by a perturbation method in a power series expansion with respect to the powers of θ_1 and θ_2 . Thus, there exists a similar solution for the Prandtl equations, leading to the conclusion of independence of the surface velocity u_s from the distance x (excluding the origin $x = 0$):

$$u_s = U_L^\infty [1 + \sqrt{\pi} \alpha \theta_2 - \alpha^2 \theta_2^2 + \sqrt{\pi} \alpha_1 \theta_1^2 \theta_2 + \theta_2^3 \varphi_2'(0)]. \quad [2]$$

The experimental investigation of these theoretical findings is of great interest, and is the purpose of this part of the paper.

2. EXPERIMENTAL APPARATUS AND MEASUREMENT

All experiments were carried out on the experimental unit shown in figure 1. Distilled water from the pump 1 and fresh air through gas blower 2 enter the horizontal channel 5, passing through the control rotameters 3 and 4. The channel was 2 m in length to 0.5 m in width. After the two distribution sets 6 and 7, the gas and the liquid interact and leave the channel at the exit, which is entirely

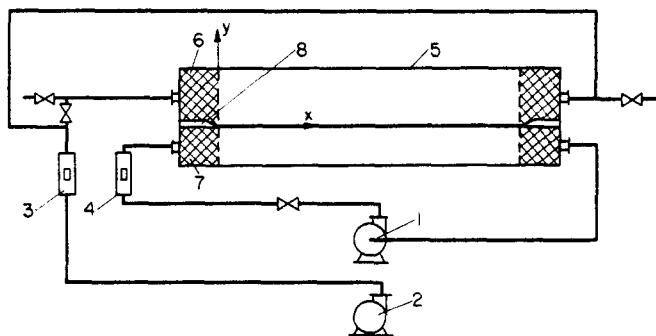


Figure 1. Sketch of the experimental apparatus.

†All indices are as in Part I.

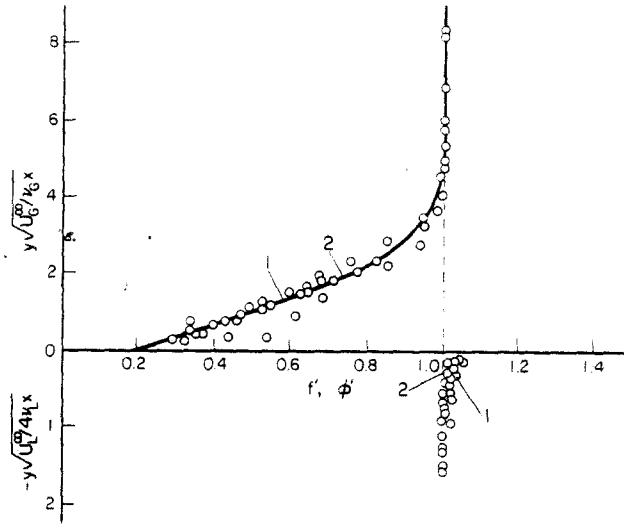


Figure 2. Theoretical (solid line) and experimental (points) velocity profiles for $\theta_1 = 0.200$ and $\theta_2 = 0.054$. Curve 1—theoretical profile obtained by the perturbation method, curve 2—theoretical profile obtained by the "exact" solution of the problem. $f'(0) = 0.206$; $\varphi'(0) = 1.031$.

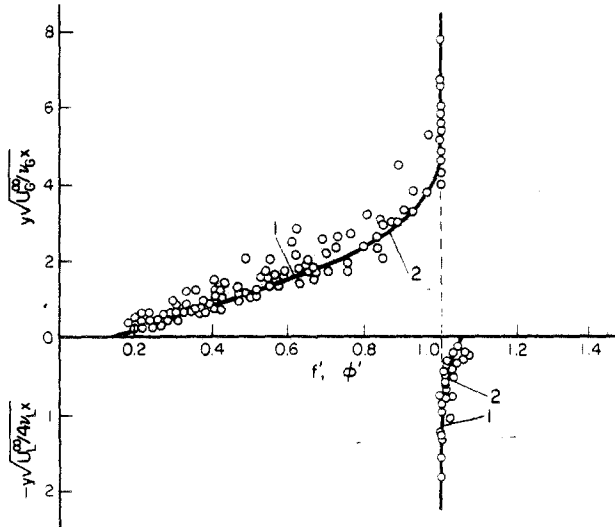


Figure 3. Theoretical (solid line) and experimental (points) velocity profiles for $\theta_1 = 0.143$ and $\theta_2 = 0.089$. Curve 1—theoretical profile obtained by the perturbation method, curve 2—theoretical profile obtained by the "exact" solution of the problem. $f'(0) = 0.150$; $\varphi'(0) = 1.051$.

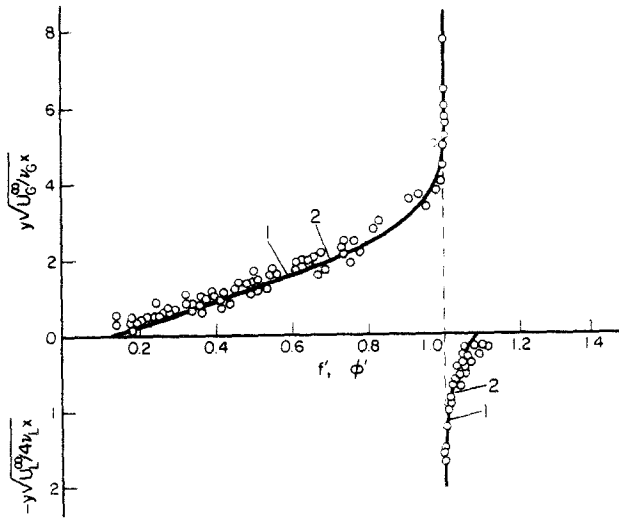


Figure 4. Theoretical (solid line) and experimental (points) velocity profiles for $\theta_1 = 0.100$ and $\theta_2 = 0.152$. Curve 1—theoretical profile obtained by the perturbation method, curve 2—theoretical profile obtained by the "exact" solution of the problem. $f'(0) = 0.109$; $\varphi'(0) = 1.087$.

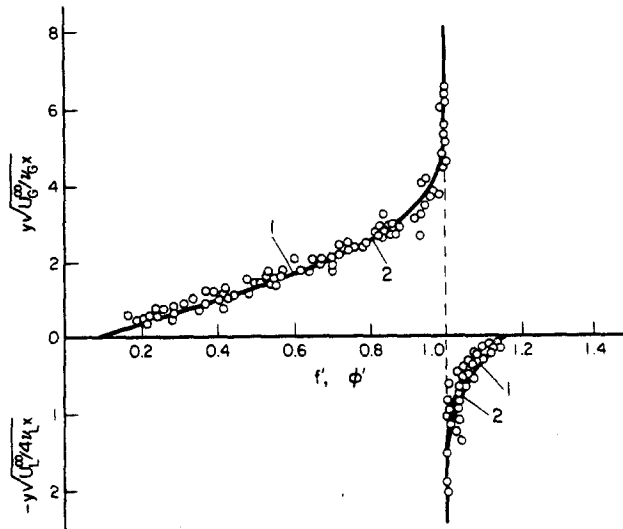


Fig. 5. Theoretical (solid line) and experimental (points) velocity profiles for $\theta_1 = 0.067$ and $\theta_2 = 0.277$. Curve 1—theoretical profile obtained by the perturbation method, curve 2—theoretical profile obtained by the “exact” solution of the problem. $f'(0) = 0.078$; $\varphi'(0) = 1.156$.

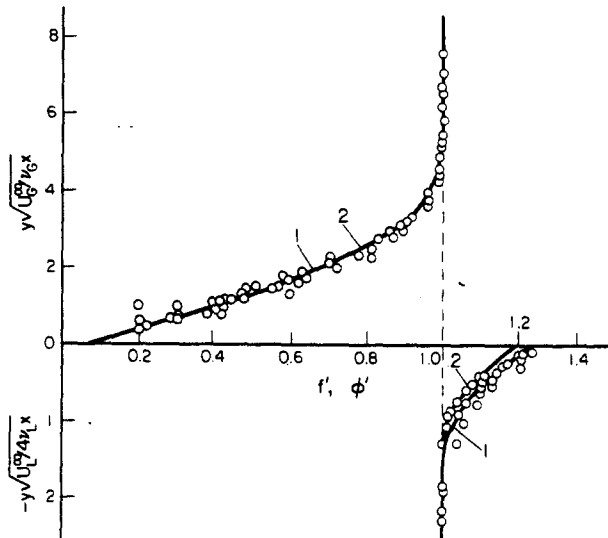


Figure 6. Theoretical (solid line) and experimental (points) velocity profiles for $\theta_1 = 0.050$ and $\theta_2 = 0.429$. Curve 1—theoretical profile obtained by the perturbation method, curve 2—theoretical profile obtained by the “exact” solution of the problem. $f'(0) = 0.063$; $\varphi'(0) = 1.232$.

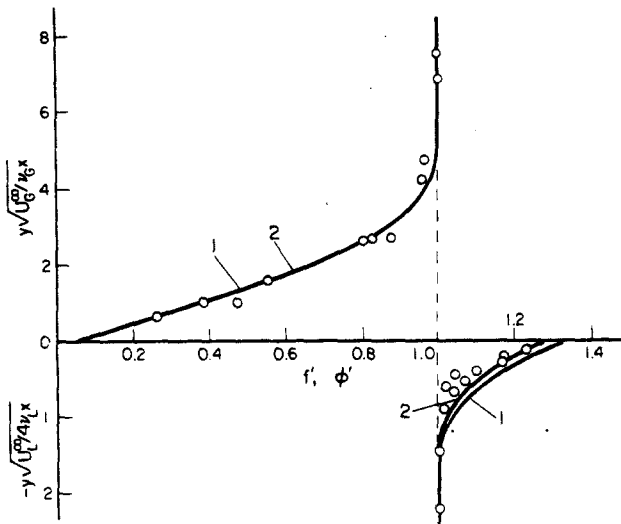


Figure 7. Theoretical (solid line) and experimental (points) velocity profiles for $\theta_1 = 0.040$ and $\theta_2 = 0.600$. Curve 1—theoretical profile obtained by the perturbation method, curve 2—theoretical profile obtained by the “exact” solution of the problem. $f'(0) = 0.054$; $\varphi'(0) = 1.314$.

symmetrical to the entrance. The rotameters 3 and 4 were used only for setting a constant flow rate during the time needed for one experiment (velocity profile measurement). The distribution sets were constructed to produce a plug velocity profile, which was specially controlled at the origin. The gas and the liquid contact at the end of the dividing edge, 8. The length of the investigated interface was 1.3 m, and the fluid depth was 0.14 m for the gas phase and 0.07 m for the liquid. Hot wire techniques were used for the velocity distribution measurements. We used DISA Thermoanemometer Type 55A01 with a Type 55A80 probe for the gas velocity measurements and a Type 55A81 for the liquid velocity measurements. The probes were carefully calibrated before each experiment on a special apparatus generating a precise Hagen–Poiseuille velocity profile.

All experiments were carried out at a constant temperature of both phases, $27 \pm 1^\circ\text{C}$. The fluid velocity was measured in the middle zone of the channel at a distance 1.5 mm; 3.0 mm; 4.5 mm; etc. from the interface in both directions until the velocities of the potential flows (U_G^∞ and U_L^∞) were reached. Six velocity ratios were investigated ($U_G^\infty = 7 + 30 \text{ cm/s}$; $U_L^\infty = 1.0 + 2.4 \text{ cm/s}$) and for each one twelve velocity profiles were obtained at 0.1; 0.2; ...; 1.2 m from the edge, 8.

3. EXPERIMENTAL RESULTS

From the experimental velocity profiles in the gas and in the liquid phase the dimensionless profiles f' and φ' by means of [1] for various values of θ_1 and θ_2 were derived. The results were compared, figures 2–7 with the theoretical curves f' and φ' obtained by the “exact” numerical solution of Prandtl’s equations and by the perturbation method as was done in Part I and Boyadjiev (1971) and Boyadjiev & Piperova (1971). The theoretical results in figures 2–7 were calculated for $\theta_2 \sqrt{(\theta_1^3)} = \text{const.}$ since the value of $(\mu_G/\mu_L)(\nu_G/\nu_L)^{-1/2}$ is practically constant in the interval $26^\circ\text{C} < t < 28^\circ\text{C}$.

The comparison of the theoretical values of the interface velocity U_s with the experimental ones U_s^E is shown in figure 8. The ratios U_s^E/U_s are calculated at a mean value for the different values of the parameter θ_2 studied.

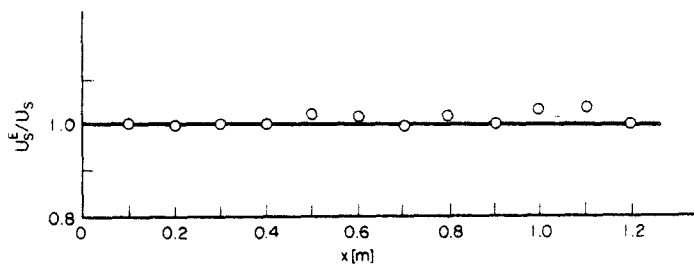


Figure 8. Comparison of the theoretical (U_s) and experimental (U_s^E) interface velocities for different distances from the interaction beginning. The value of U_s^E/U_s (points) is average for the six values of θ_2 studied.

4. CONCLUSION

An experimental measurement of the velocity profiles at the interface of two-phase co-current flows was carried out. The theoretical results show that the velocity profiles calculated by means of the perturbation theory are in a good agreement with the results obtained by an accurate numerical “exact” solution of the boundary layer problem. The experimental data confirm their validity. Thus, they can be used for calculation of the velocity distribution in the laminar boundary layers at a moving interface for co-current gas–liquid stratified flow.

REFERENCES

- BOYADJIEV, CHR., MITEV, PL. & SAPUNDZHIEV, T. 1976 Laminar boundary layers of co-current gas–liquid stratified flows—I. Theory. *Int. J. Multiphase Flow* 3, 51–55.
- BOYADJIEV, CHR. 1971 The hydrodynamics of certain two-phase flows. 1. The laminar boundary layer at a flat gas–liquid interface. *Int. Chem. Engng* 11, 464–469.
- BOYADJIEV, CHR. & PIPEROVA, M. 1971 The hydrodynamics of certain two-phase flows. 4. Evaluation of some special functions. *Int. Chem. Engng* 11, 479–487.